Contribution from the Research School of Chemistry,
Australian National University, Canberra, ACT 2600, Australia

# Electrochemistry of Macrobicyclic Mixed Nitrogen–Sulfur Donor Complexes of Cobalt(III)

LAWRENCE R. GAHAN,[1a] GEOFFREY A. LAWRANCE,[1b] and ALAN M. SARGESON*

The redox chemistry of the mixed nitrogen–sulfur donor cobalt(III) complexes with the macrobicyclic ligands 8-methyl-6,10,19-trithia-1,3,14,16-tetraazabicyclo[6.6.6]icosane (azacapten), 1-methyl-8-nitro-3,13,16-trithia-6,10,19-triazabicyclo[6.6.6]icosane ((NO₂)capten), and 8-ammonio-1-methyl-3,13,16-trithia-6,10,19-triazabicyclo[6.6.6]icosane ((NH₃⁺)capten) and of the hexadentate precursor ligand 5-(4-amino-2-thiabutyl)-5-methyl-3,7-dithia-1,9-nonanediamine (ten) has been investigated in aqueous and aprotic solutions. The macrobicyclic complexes exhibit a chemically and electrochemically reversible Co(III)/Co(II) couple near 0 V in aqueous (NHE) and aprotic solutions (Ag/AgCl) and a chemically irreversible but elctrochemically reversible 1-e couple near −1 V, nominally Co(II)/Co(I). In addition, a further multielectron couple is observed for the azacapten complex at more negative potentials. No evidence for oxidation processes was forthcoming. The low-spin d^7 cobalt(II) complex of (NH₃⁺)capten has been characterized by ESR spectroscopy at 4.2 K, and the nominally d^8 cobalt(I) complex, at 100 K. The former compound exhibits *g* values at 1.94, 2.21, and 4.22, while the latter compound shows an eight-line pattern at *g* = 2.17 (*A* = 67 G) consistent with its formulation as d^8 Co(I) and not as a d^7 Co(II)–S radical state.

Introduction

Synthetic routes to macrobicyclic hexaamine complexes of cobalt(II) have been reported.[2,3] As a consequence of encapsulation, the normally rapid substitution chemistry of cobalt(II) does not occur and chemical and electrochemical reversibility is observed for the cobalt(III)/cobalt(II) couple in a wide range of complexes of type I. However, irreversible
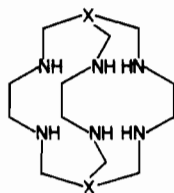
I: X = N, C—NO₂, C—NH₂, C—Cl...

reduction with rupture of the cage invariably occurs for the cobalt(II) form of the encapsulated complexes.[4] Although there is evidence for stable cobalt(I) species in macro-monocyclic amine complexes,[5] the tight cage structure in the 20-membered bicyclo[6.6.6]icosane macrobicycles apparently does not have a cavity size sufficiently large to accommodate cobalt(I). Energy minimization calculations suggest the cavity size in these ligands is optimum for an ion size intermediate between that of Co³⁺ and Co²⁺.[6] Larger ions such as Co⁺ and Co⁰ are not accommodated, and so far the irreversible reduction of the cobalt(II) hexaamines (I) and rupture of the cage are consistent with this.

Recently, syntheses of macrobicyclic complexes of cobalt(III) with mixed nitrogen–sulfur donor atoms have been reported.[7] The ions [8-methyl-6,10,19-trithia-1,3,14,16-tet-

II   IIIa, R = NO₂   IV
            IIIb, R = NH₃⁺
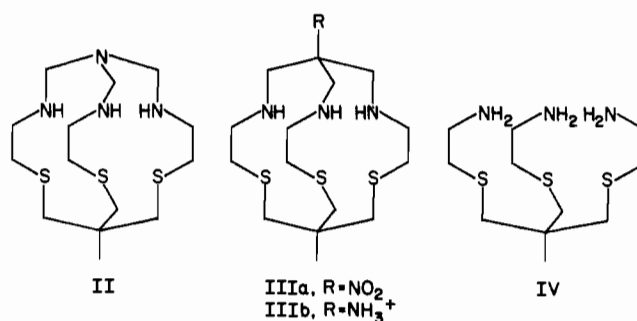
raazabicyclo[6.6.6]icosane]cobalt(III), Co(azacapten)³⁺ (II), [1-methyl-8-nitro-3,13,16-trithia-6,10,19-triazabicyclo-[6.6.6]icosane]cobalt(III), Co((NO₂)capten)³⁺ (IIIa), and [8-ammonio-1-methyl-3,13,16-trithia-6,10,19-triazabicyclo-[6.6.6]icosane]cobalt(III), Co((NH₃⁺)capten)⁴⁺ (IIIb), have been prepared from the hexadentate precursor 5-(4-amino-2-thiabutyl)-5-methyl-3,7-dithia-1,9-nonanediamine, Co(ten)³⁺ (IV). As a consequence of the longer Co–S and S–C bonds compared with Co–N and C–N analogues, the effective cavity is somewhat larger than in the hexaamine analogues (I); further, thioether donors are "softer" than amine donors, and they may augment the stability of the lower oxidation states. The electrochemistry of these mixed-donor complexes has now been investigated.

Experimental Section

Syntheses of the complex [Co(ten)]Cl₃ and of the macrobicyclic complexes [Co(azacapten)]³⁺, [Co((NO₂)capten)]³⁺, and [Co-((NH₃⁺)capten)]⁴⁺ have been described elsewhere.[7] Complexes were isolated as the perchlorate or trifluoromethanesulfonate (triflate) salts and were analytically pure.

Sodium perchlorate (AR grade) or tetramethylammonium trifluoromethanesulfonate (TMAT) were used as electrolytes for electrochemical studies in aqueous and nonaqueous solutions, respectively, usually at 0.1 M ionic strength. Double-glass-distilled water and dried AR grade acetone and acetonitrile were employed as solvents for electrochemistry.

Electrochemistry. Experiments were performed on a Princeton Applied Research Model 170 electrochemistry system and a standard three-electrode configuration with positive-feedback *iR* compensation. Rapid-scan voltammetry was performed with the aid of a Tektronix 5031 oscilloscope and Tektronix C70 oscilloscope camera attachment. Saturated (KCl) calomel (SCE) (aqueous solutions) or silver–silver

(1) Present addresses: (a) Chemistry Department, University of Queensland, St Lucia, QLD 4067, Australia. (b) Chemistry Department, The University of Newcastle, NSW 2308, Australia.
(2) Creaser, I. I.; Harrowfield, J. M.; Herlt, A. J.; Sargeson, A. M.; Springborg, J.; Geue, R. J.; Snow, M. R. *J. Am. Chem. Soc.* **1977**, *99*, 3181.
(3) Creaser, I. I.; Geue, R. J.; Harrowfield, J. M.; Herlt, A. J.; Sargeson, A. M.; Snow, M. R.; Springborg, J. *J. Am. Chem. Soc.* **1982**, *104*, 6016. See also: Sargeson, A. M. *Chem. Br.* **1979**, *15*, 23.
(4) Bond, A. M.; Lawrance, G. A.; Lay, P. A.; Sargeson, A. M. *Inorg. Chem.* **1983**, *22*, 2010.
(5) Tait, A. M.; Lovecchio, F. V.; Busch, D. H. *Inorg. Chem.* **1977**, *16*, 2206 and references therein.
(6) Geue, R. J., personal communication of unpublished data.
(7) Gahan, L. R.; Hambley, T. W.; Sargeson, A. M.; Snow, M. R. *Inorg. Chem.* **1982**, *21*, 2699.
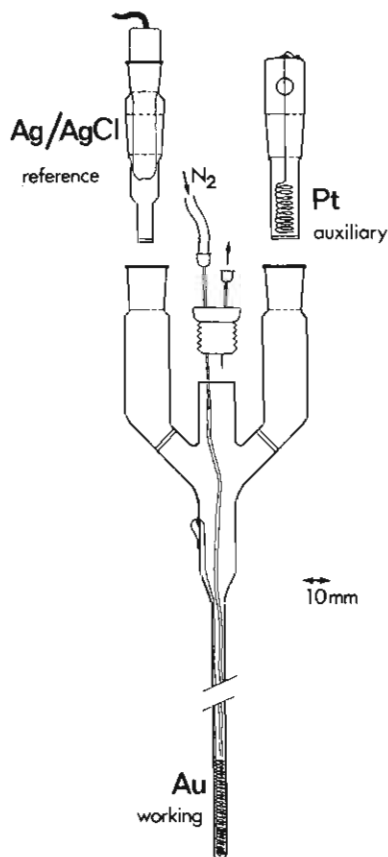
Figure 1. Schematic diagram of the "in situ" electrochemical ESR cell.

chloride/saturated LiCl in acetone (nonaqueous solutions) reference electrodes were used, separated from the working compartment by a fine-porosity glass frit. The auxiliary electrode was a platinum coil. Polarography was performed with a standard dropping-mercury working electrode assembly (DME), while voltammetry employed a hanging-mercury-drop (HMDE) or platinum-button working electrode. Solutions were deoxygenated with solvent-saturated high-purity argon through a standard purge tube. Coulometry was performed with a PAR Model 377 cell at a mercury pool, using an Amel Model 551 potentiostat and Amel Model 731 digital integrator. Throughout, concentrations of complexes were usually in the millimolar range.

Spectroscopy. Electron spin resonance (ESR) spectra were recorded with a JEOL JES-PE or a Varian V-4502 spectrometer. The NH_3^+-capped cobalt(II) complex was prepared in solution by chemical reduction with zinc amalgam and transferred and sealed in an ESR tube under a nitrogen atmosphere. The spectrum was recorded of a frozen glass at 4.2 K with use of a liquid-helium flow cryostat. The (NH_3)capten cobalt(I) complex was generated in situ in an electrochemical ESR cell of our own design by electrolysis of a solution of the complex (~5 mM) in acetonitrile at −60 °C and −1.3 V (vs. Ag/AgCl). Subsequent rapid cooling to 100 K allowed the reduced ion to be trapped and its spectrum to be recorded in a frozen glass.

The electrochemical ESR cell contained a fine-gold-coil working electrode in the base of the tube, wound as a low-pitch coil of 16 turn/cm, as previously described.[8] This configuration allows, if required, electrolysis and signal recording simultaneously. The cell also carried a platinum-coil auxiliary electrode and a Ag/AgCl reference electrode, separated from the working compartment by double glass frits. Provision for degassing via a narrow (21 gauge) flexible tube and inlet and outlet needles in a suba-seal cap was provided. The cell is shown schematically in Figure 1.

Spectroelectrochemistry of the (NH_3^+)capten complex was attempted with a cell fitted with a gold minigrid working electrode in the light path (2 mm) and Pt coil and Ag/AgCl auxiliary and working electrodes, respectively. Complete electrolysis in this type of cell is

(8) Allendoerfer, R. D.; Martinchek, G. A.; Bruckenstein, S. *Anal. Chem.* **1975**, *47*, 890.
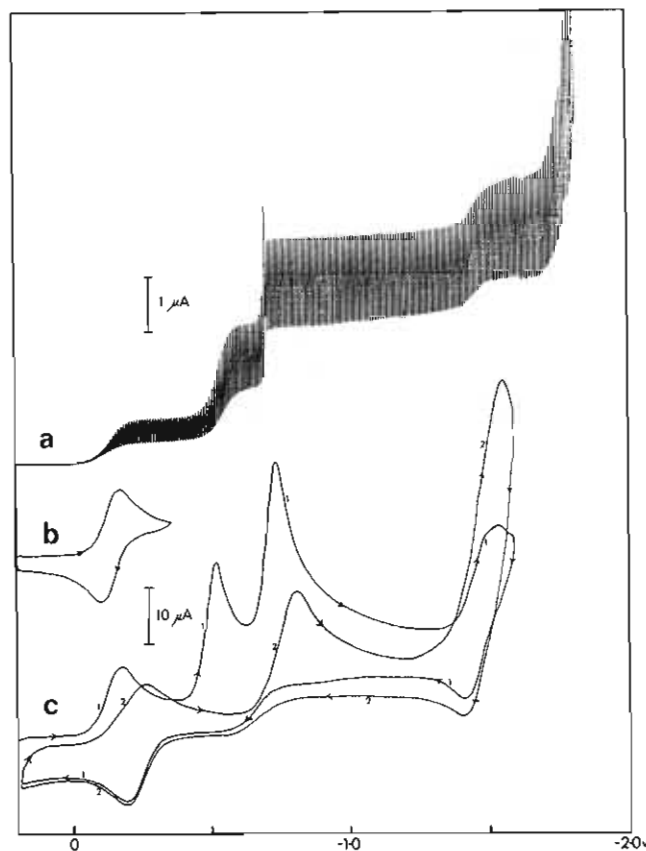
Figure 2. Voltammetry of $Co((NO_2)capten)^{3+}$ in aqueous solution (1 mM complex, 0.1 M $NaClO_4$): (a) dc polarogram (1/2-s drop time; 20 mV/s scan speed); (b) cyclic voltammogram (HMDE; scan rate 500 mV/s; switching potential −0.35 V); (c) repeat scan cyclic voltammogram (HMDE; scan rate 500 mV/s; switching potential −1.6 V).

on the minutes time scale, which proved inadequate in this case due to the chemical instability of the lower oxidation state product. Shorter path length cells where electrolysis is more rapid were inadequate due to the small molar absorbtivities of precursor and product.

Results

Aqueous Electrochemistry. All complexes studied showed an electrochemically reversible Co(III)/Co(II) couple near 0 V (Table I). This behavior is consistent with the established chemical reversibility of the couple, where both the connectivity of the cobalt(III) cage and its chirality are fully retained throughout chemical reduction and subsequent reoxidation.[7] The 1-e nature of the couple was confirmed coulometrically for $Co(azacapten)^{3+}$ and $Co((NH_3^+)capten)^{4+}$. In aqueous solution at ambient temperature, the determined E values for the Co(III)/Co(II) couple were +0.06 V (ten), +0.01 V (azacapten), +0.10 V ((NO_2)capten), and +0.06 V ((NH_3^+)capten) vs. the normal hydrogen electrode at $\mu = 0.1$ M. Further reductions were observed in each complex in aqueous solution at more negative potentials than that of the Co(III)/Co(II) couple (Table I).

The (NO_2)capten complex exhibited a dc polarogram complicated by waves from stepwise irreversible reduction of the nitro group (Figure 2). Each irreversible step is apparently two electron in nature as deduced from the dc wave height comparisons. These waves were absent from the dc polarogram of the fully reduced (NH_3^+)capten complex. Coulometry in neutral solution confirmed that the nitro group is reduced to the hydroxylamine (4-e reduction) rather than to the amine group (6-e reduction); the latter reduction was achieved chemically with zinc in aqueous acid. A further wave was observed near −1.5 V, assigned from dc and derivative-pulse
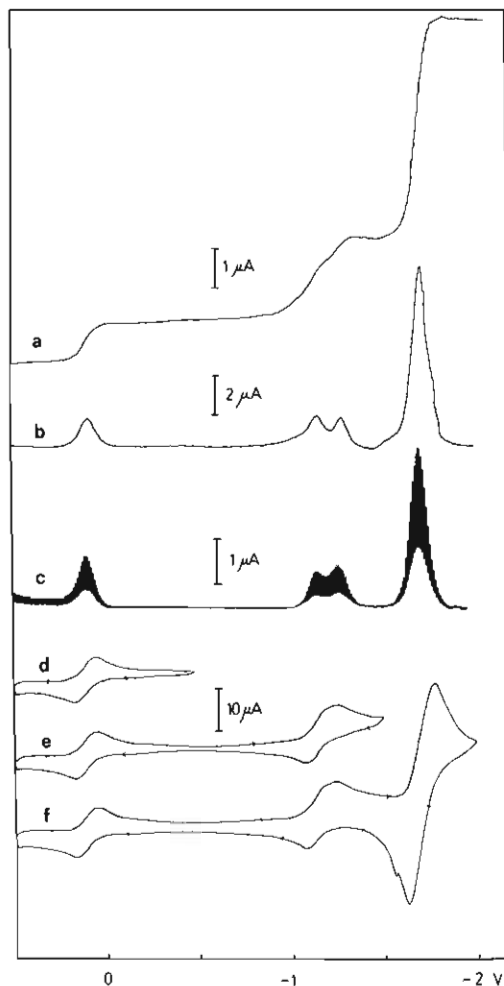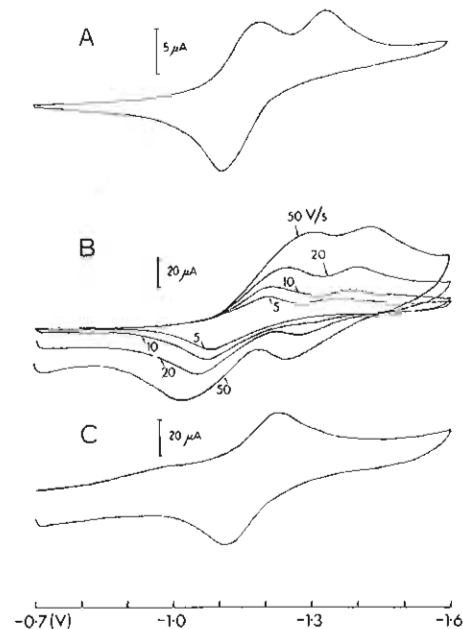
Figure 3. Voltammetry of Co(azacapten)$^{3+}$ in acetonitrile (1 mM complex, 0.1 M Me$_4$NOSO$_2$CF$_3$): (a) current-sampled dc polarogram (1/2-s drop time; 20 mV/s scan rate; 10-ms sampling time); (b) derivative-pulse polarogram (ΔE = 50 mV; 1-s drop time; 5 mV/s scan speed); (c) ac polarogram (ω = 400 Hz; ΔE = 5 mV (PP); 1/2-s drop time; 20 mV/s scan speed); (d–f) cyclic voltammograms (HMDE; 500 mV/s) with switching potentials of –0.5, –1.5, and –2.0 V, respectively.

Figure 4. Cyclic voltammetry of Co(azacapten)$^{3+}$ in acetone solution (1 mM complex, 0.1 M Me$_4$NOSO$_2$CF$_3$): (A) HMDE, scan rate 1 V/s; (B) HMDE, scan rate variable 5–50 V/s; (C) stationary Pt billet, scan rate 1 V/s.

Figure 5. Variable-frequency in-phase ac peak current (I_{peak}) of all four signals observed in the ac polarogram of Co(azacapten)$^{3+}$ (DME; 1/2-s drop time; ΔE = 5 mV (PP); 20 mV/s scan speed; acetonitrile solvent; 2 mM complex; 0.1 M Me$_4$NOSO$_2$CF$_3$): (A) Co(III)/Co(II) couple; (B) Co(II)/Co(I) couple; (C) associated adsorption wave; (D) ligand-centered multielectron reduction.

polarograms as a 1-e couple, nominally Co(II)/Co(I). Repeat scan cyclic voltammetry (Figure 2c) illustrates the irreversible nature of the nitro group reduction, and a shift in the cathodic maximum for the Co(III)/Co(II) couple from –0.17 V (first scan) to –0.27 V (second scan) is consistent with the formation of a complex with a different capping group (–NHOH rather than –NO$_2$).

For the (NH$_3$$^+$)capten complex, variable-frequency in-phase ac polarography (ω = 10–1100 Hz) showed a linear dependence of peak height vs. $\omega^{1/2}$, indicative of a rapid heterogeneous electron-transfer rate (k_{el}).[9] Analogous hexammine macrobicyclic complexes show significant curvature of such plots at high frequencies, due to a slower electron-transfer rate.[4] Apart from the Co(III)/Co(II) couple, the dc polarogram showed a composite apparently 2-e wave near –1.4$_5$ V. This latter wave had two separate maxima (–1.38 and –1.52 V) in the derivative-pulse polarogram. Since an ac signal in this region occurred at the more positive potential only, it was assigned to the Co(II)/Co(I) couple and the remaining wave to an irreversible reduction f the proton of the NH$_3$$^+$ capping group. The assignment was confirmed by cyclic voltammetry, with reversible couples at –0.19 and –1.38 V in addition to an irreversible wave at more negative potential.

The dc polarogram of Co(azacapten)$^{3+}$ was unusual. Apart from the Co(III)/Co(II) couple, a large multielectron ($n \sim$ 5–7) reduction wave was observed at –1.46 V, near the solvent limit. The small size of the ac signal ($<I_{peak}$ for the Co(III)/Co(II) couple) and the observation of an anodic peak in the cyclic voltammograms only at high speeds ($>$1 V), with $i_{pc}/i_{pa} \gg 1$, are indicative of very limited reversibility for this multielectron reduction, which is probably associated with sulfur chemistry.

Nonaqueous Electrochemistry. In acetonitrile, the dc polarogram of Co(azacapten)$^{3+}$ exhibited a 1-e reversible reduction at +0.08 V (vs. Ag/AgCl), a complex wave near –1.2 V, and a multielectron reduction near –1.7 V (Figure 3). The behavior in acetone was similar (Tables II and III). The composite wave was examined by rapid-scan cyclic voltammetry; only at scan speeds $>$20 V/s was there an indication

(9) Smith, D. E. In "Electroanalytical Chemistry"; Bard, A. J., Ed.; Marcel Dekker: New York, 1966; Vol. 1, Chapter 1.

Table I. Electrochemical Data for Mixed Thioether–Amine Complexes in Aqueous Solution[a] vs. SCE

compd	process	dc $E_{1/2}$, V	dc $(E_{1/4} - E_{3/4})$, mV	dc i_d[b]	cyclic dc E_{pc}, V	cyclic dc E_{pa}, V	cyclic dc ΔE,[c] mV	cyclic dc $E_{1/2}$, V	cyclic dc i_{pc}/i_{pa}	ac E_p,[d] V	ac $\Delta E_{1/2}$, mV	derv pulse E_p,[e] V	derv pulse $\Delta E_{1/2}$, mV	coulometry n
Co(ten)³⁺	Co III/II	−0.22	70	1.0	−0.26	−0.14	120	−0.20	0.9	−0.24[f]	100	−0.22	110	1.0
	Co II/0	−1.02	30	2.0	−1.06	abst				−1.06	65	−1.03	70	1.9
Co(azacapten)³⁺	Co III/II	−0.23	56	1.0	−0.265	−0.198	67	−0.23	1.0₅	−0.18[f]		−0.24	95	1.0
	multielectron	−1.43₅	38	4.7	−1.45	abst[g]				−1.46	100	−1.47[h]	60	
Co((NH₃⁺)capten)⁴⁺	Co III/II	−0.18	56	1.0	(−0.27) / −0.20	−0.18 / −0.125	90 / 75	−0.22₅ / −0.16	1.0₅[j] / 1.0₅	−0.14[f]	100	−0.18₅	92	1.0
	Co II/I	−1.3₅		1.2	−1.38	abst				−1.33		−1.38	100	
	H⁺ redn	−1.5		1.1	−1.56	abst				abst		−1.52[i]	100	
Co(NO₂)capten³⁺	Co III/II	−0.14₅	56	1.0	(−0.22₅) / −0.17₅	−0.12₅ / −0.11	100 / 65	−0.17₅ / −0.14	1.0[j] / 1.0₅	−0.13[f]	95	−0.16	95	1.0
	NO₂ → NO	−0.55	45	1.9	−0.50	abst				−0.57		−0.57	80	
	NO → NHOH	−0.71₅		1.9₅	−0.72	abst				−0.71		−0.72	100	
	Co II/I	−1.48	58	1.0	−1.51	−1.41	100	−1.46	1.1	−1.46		−1.49	100	4.0[k]

[a] 0.1 M NaClO₄; ambient temperature; DME unless otherwise specified, with 0.5-s drop time and scan rates of 20 mV/s (dc and ac), 10 mV/s (derivative pulse), and 100 mV/s (cyclic dc). [b] Relative diffusion currents, based on i_d of 1.0 for the Co(III)/Co(II) couple. [c] ΔE and $E_{1/2}$ values determined with switching potentials more positive than other irreversible waves. [d] $\omega = 200$ Hz; $\Delta E_{pp} = 10$ mV. [e] $\Delta E = 25$ mV (pp). [f] Complicated by adsorption phenomena. [g] An anodic wave is observed only at scan rates >10 V/s. [h] Peak current seven times that of the Co(III)/Co(II) couple. [i] Cyclic voltammetry at stationary Pt, 500 mV/s. [j] Peak current of all three waves approximately equal. [k] Controlled potential of −0.8 V in this case; other coulometry at 200 mV more negative than $E_{1/2}$.

Table II. Electrochemical Data for Mixed Thioether–Amine Complexes in Acetonitrile[a] vs. Ag/AgCl (0.1 M LiCl in Acetone)

compd	process	dc $E_{1/2}$, V	dc $(E_{1/4} - E_{3/4})$, mV	dc i_d[b]	cyclic dc E_{pc}, V	cyclic dc E_{pa}, V	cyclic dc ΔE,[c] mV	cyclic dc $E_{1/2}$, V	cyclic dc i_{pc}/i_{pa}	ac E_p,[d] V	ac $\Delta E_{1/2}$, mV	derv-pulse E_p,[e] V	derv-pulse $\Delta E_{1/2}$, mV	coulometry n
Co(ten)³⁺	Co III/II	+0.23	80	1.0	+0.14	+0.29	150	+0.21₅	0.8	+0.20	100	+0.23	110	1.0
	Co II/I	−0.72	52	1.6	−0.83	abst				−0.76	150	−0.71	95	1.9
	multielectron	−2.3₅[f]			−2.3[d]	abst				−2.4[h]		−2.3		
Co(azacapten)³⁺	Co III/II	+0.09₅	58	1.0	+0.06	+0.15	90	+0.09₅	1.0	+0.09₅	90	+0.08	90	1.0
	Co II/I	−1.15[h]	~160	1.8	−1.20	−1.08	120	−1.14	1.0	−1.15	~100	−1.16	~110	1.2
	multielectron	−1.70	63	5.7	−1.75	−1.64	110	−1.69₅	1.6	−1.26[i]	~100	−1.28	~100	
					0.00	+0.20	200	+0.10	~1[j]					
					−1.18	−1.06	120	−1.12	~1	−1.70	100	−1.72	100	
					−1.67	abst								
Co((NH₃⁺)capten)⁴⁺	Co III/II	+0.30	56	1.0	+0.34₅	+0.24₅	90	+0.30	1.0	+0.30	95	+0.28₅	90	1.0[l]
	Co II/I	−0.89[k]	59	1.0₅	−0.95	−0.85	100	−0.90	1.1	−0.90	105	−0.92	100	1.1[l]
	H⁺ redn	~−1.5[k]			−1.57	abst				−1.56				
Co(NO₂)capten³⁺	Co III/II	+0.21	56		+0.175	+0.265	90	+0.22	1.0	+0.215	95	+0.20	95	1.0
					+0.16	+0.28	120	+0.22	1.0[j]					
	mixed	~−1.3[m]			~−1.0₅	abst				−1.4₅	140	−1.06[n]		
					~−1.3	abst						~−1.4[o]		
					−1.18	abst								
					−1.5	abst								

[a] 0.1 M Me₄NCF₃SO₃; ambient temperature; DME unless otherwise stated, with 0.5-s drop time and scan rates of 20 mV/s (dc and ac), 10 mV/s (derivative pulse), and 200 mV/s (cyclic dc). [b] Relative diffusion currents, based on i_d of 1.0 for the reversible Co(III)/Co(II) couple. [c] ΔE and $E_{1/2}$ values determined with switching potentials more positive than other irreversible waves. [d] $\omega = 200$ Hz; $\Delta E_{pp} = 10$ mV. [e] $\Delta E = 25$ mV. [f] Shoulder on solvent front. [g] i_{pc} ratios of 1:1.3:6 for the three waves. [h] Complicated by adsorption. [i] Clearly characterized as an adsorption wave from phase-sensitive and variable-frequency ac polarography. [j] Determined at −60 °C. [k] Adsorption superimposed. [l] Determined at −60 °C. [m] Extremely broad wave, covering NO₂ and metal-centered reduction region. [n] Adsorption spike. [o] Broad.

Table III. Electrochemical Data for Mixed Thioether-Amine Complexes in Acetone[a] vs. Ag/AgCl (0.1 M LiCl in Acetone)

		dc			cyclic dc					ac		derv pulse	
compd	process	$E_{1/2}$, V	$(E_{1/4}-E_{3/4})$,[b] mV	i_d[b]	E_{pc}, V	E_{pa}, V	ΔE_c,[c] mV	$E_{1/2}$, V	i_{pc}/i_{pa}	E_p,[d] V	$\Delta E_{1/2}$, mV	E_p,[e] V	$\Delta E_{1/2}$, mV
Co(ten)³⁺	Co^{III}/II	+0.05	70	1.0	0.01	+0.07	80	+0.03	1.0	+0.03	100	+0.06	110
	Co^{II}/I	−1.22	80	1.1	−1.20	abst	120	+0.03	1.0[f]	−1.22	120	−1.23	180
					−0.03	+0.09							
					−1.2	abst							
Co(azacapten)³⁺	Co^{III}/II	+0.04	56	1.0	+0.085	+0.005	80	+0.04	1.0	+0.04	90	+0.03	90
	Co^{II}/I	−1.12[g]	~100	1.7	−1.19	−1.11	80	−1.15	1.0	−1.13	95	−1.14	95
					−1.34[h]	abst	120	−1.73	1.5	−1.30[i]	140	−1.25	
	multielectron	−1.73	~50	3.6	−1.79	−1.67	140	+0.02	1.0[f]	−1.7	120	−1.75	95
					−0.05	+0.09	110	−1.15$_s$	1.0				
					−1.22	−1.11			1.0$_s$				
Co((NH₃⁺)capten)⁴⁺	Co^{III}/II	+0.15	56	1.0	+0.11	+0.19	80	+0.15$_s$	1.0$_s$	+0.15$_s$	95	+0.14	90
	Co^{II}/I	−1.03	58	1.1	−1.08	−1.00	80	−1.04	1.0[f]	−1.15	110	−1.04	100
	H⁺ redn	−1.45$_s$	78	1.1	−1.47	abst	180	+0.15	~1	−1.39	180	−1.48	170
Co((NO₂)capten)³⁺	Co^{III}/II	+0.135	56	1.0	+0.06	+0.24	160	−1.12	1.0	+0.15	95	+0.13	95
	mixed[j]	~-1.3		~5	−1.20	−1.04	75	+0.14	1[f]	~-1.4	180	~-1.4	160
					+0.10	+0.175	190	+0.135					
					~-1.4	abst							
					~-1.5	+0.23							
						abst							

[a] 0.1 M Me₄NCF₃SO₃; ambient temperature; DME unless otherwise stated, with 0.5-s drop time and scan rates of 20 mV/s (dc and ac), 10 mV/s (derivative pulse), and 200 mV/s (cyclic dc). [b] Relative diffusion currents, based on i_d of 1.0 for the reversible Co(III)/Co(II) couple. [c] ΔE and $E_{1/2}$ values determined with switching potentials more positive than other irreversible couples. [d] $\omega = 200$ Hz. [e] $\Delta E = 10$ mV. [f] Cyclic at stationary Pt; scan rate 500 mV/s. [g] $\Delta E = 25$ mV (pp). [h] Adsorption wave, absent in cyclics at Au or Pt working electrodes. [i] Clearly characterized as an adsorption wave by phase-sensitive and variable-frequency ac polarography. [j] Extremely broad wave, covering the NO₂ reduction and metal-centered reduction region.
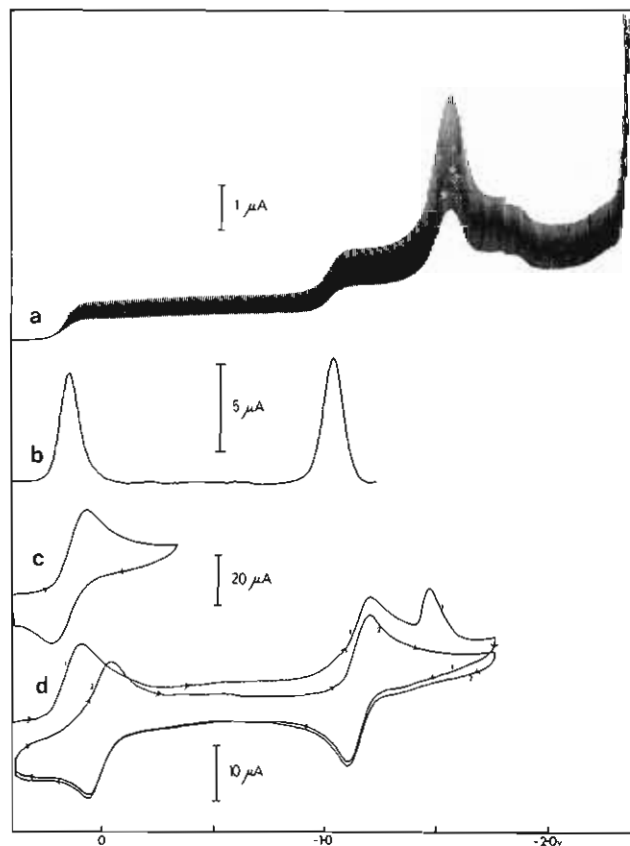

Figure 6. Voltammetry of Co((NH₃⁺)capten)⁴⁺ in acetone (1 mM complex, 0.1 M Me₄NOSO₂CF₃): (a) dc polarogram (1/2-s drop time; 20 mV/s scan rate); (b) derivative-pulse polarogram ($\Delta E = 50$ mV; 1-s drop time; 5 mV/s scan speed); (c) cyclic voltammogram at a stationary Pt billet (scan rate 10 mV/s); (d) repeat scan cyclic voltammogram at a HMDE (500 mV/s scan speed).

of two cathodic and two anodic waves at the HMDE (Figure 4). At a platinum electrode, only one cathodic and one anodic wave was observed at all scan rates. This behavior implies some specific adsorption interaction at the mercury electrode. For ac polarograms (Figure 3c), variable patterns were observed for each peak when in-phase current peak height was plotted against $\omega^{1/2}$ (Figure 5). A linear dependence for the initial reversible Co(III)/Co(II) couple is consistent with a relatively large heterogeneous electron-transfer rate constant, k_{el}. A plot of approximately the same limiting slope was observed for the second wave, assigned to the 1-e Co(II)/Co(I) couple. The complex frequency dependence of the third wave implies an adsorption process at the mercury electrode, and this conclusion is supported by the phase-sensitive ac polarographic behavior. The multielectron reduction showed typical quasi-reversible behavior, with a limiting slope approximately five times that of the first 1-e couple. The latter wave was not observed for any other complex before the solvent limit.

The dc polarogram of Co((NO₂)capten)³⁺ in aprotic solvents showed very broad waves spanning over 1 V associated with irreversible nitro group reduction. This pattern is typical of nitro group reduction in aprotic solvents when no ready proton source is available. Reduction to nitro radicals and subsequent reaction of these radicals have been implicated in the analogous hexaamine complex electrochemistry.[4] Coulometry in acetone also indicated a 1-e reduction to the nitro radical, followed by irreversible chemical processes that were not pursued.

The behavior of the (NH₃)capten complex was quite simple (Figure 6). Two dc waves of equal height near +0.1 and −1 V precede an adsorption maximum near −1.5 V. The latter maximum is presumably associated with proton reduction on the NH₃⁺ capping group. Cyclic voltammetry at the HMDE

1000

4000 G

400 G
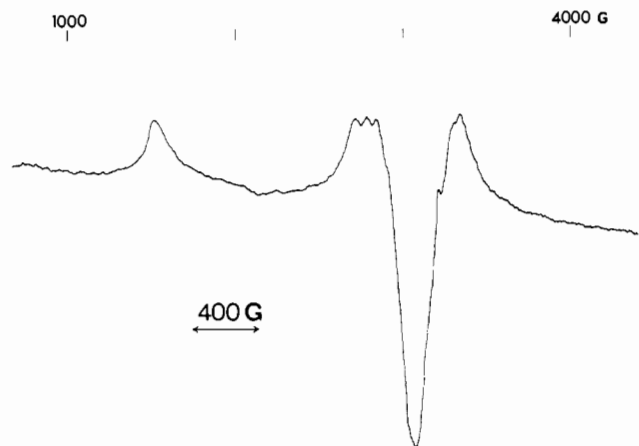
Figure 7. X-Band ESR spectrum of Co((NH$_3^+$)capten)$^{3+}$ (d^7 cobalt(II)) as a frozen aqueous solution recorded at 4.2 K and 8.51 GHz.

A

B

100 G

$\frac{H}{\text{incr.}}$

Figure 8. X-Band ESR spectrum of the nominally d^8 cobalt(I) complex of (NH$_3^+$)capten recorded at 100 K as a frozen glass following in situ generation at 210 K in acetonitrile. Spectra are (A) reduced cobalt solution and (B) solvent blank, both treated in the same manner.

(Figure 6d) is consistent with this assignment. The derivative-pulse dc wave heights for the first two reductions were identical (Figure 6b), and the 1-e nature of these two steps was confirmed coulometrically. However, the nominal Co(I) product of the controlled-potential electrolysis at −1.2 V could not be reoxidized quantitatively to the precursor complex.

For all complexes, cyclic voltammetry performed at Pt or Au electrodes yielded essentially the same behavior as that reported at Hg. Peak-to-peak separations in cyclic voltammograms were electrode dependent, being generally greater on Pt and Au than on Hg, even with freshly cleaned surfaces. This parallels the behavior of the hexaamine cages, where k_{el} was less at Pt than Hg.[4] No waves were observed for any complex at potentials more anodic than the Co(III)/Co(II) couple when scanning up to +2.0 V in acetonitrile at a Pt electrode. Therefore, no evidence for accessible Co(IV) species was forthcoming.

Spectroscopy. The observation of two 1-e steps in the reduction of the Co^{III}N$_3$S$_3$ complexes implies the formation of a cobalt(I) ion and led us to attempt to characterize this species spectroscopically. The simple electrochemistry of the Co-((NH$_3^+$)capten)$^{4+/3+/2+}$ system in aprotic solvents focused our attention on this ion. The extreme sensitivity of reduced forms of the complex to oxygen was overcome by either chemical reduction in Schlenk-type apparatus in an inert gas atmosphere or by generation in situ in specially constructed cells. The cobalt(II) and Cobalt(I) complexes were prepared for ESR study by these methods respectively; since the latter species is not chemically stable at room temperature for any appreciable period, electrolysis had to be performed at low temperature.

The ESR spectrum of the d^7 cobalt(II) complex Co-((NH$_3^+$)capten)$^{3+}$, recorded at 4.2 K, is shown in Figure 7. It yields g values of 1.94, 2.21, and 4.22. At liquid-nitrogen temperatures, the signal was too broad to be adequately characterized.

The ESR spectrum of the nominally d^8 cobalt(I) complex Co((NH$_3^+$)capten)$^{2+}$, recorded at 100 K, is shown in Figure 8 and compared with a solvent blank recorded under near identical conditions. An eight-line pattern centered at g = 2.17 with a coupling of A = 67 G was observed. No further signals specific to the complex ion could be detected, since the large background of the cell at higher g values precluded observation of any weak signals in that region. The macrobicyclic nature of the ligand presumably forces the complex to retain its essentially sexidentate, monomeric environment. However, the nominally cobalt(I) state could also be represented as a cobalt(II)–thioether radical species. Analysis of this point is deferred to the Discussion section.

Attempts to record the absorption spectrum of the nominally
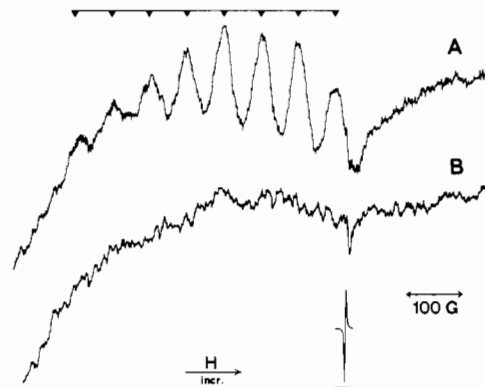
cobalt(I) ion in a spectroelectrochemical cell were frustrated by the limited chemical stability of that complex toward decomposition at accessible temperatures (>−50 °C) by apparent cage rupture and by the intensity of charge-transfer bands associated with the thioether functional groups. While the reported spectrum of the cobalt(II) complex[7] could be reproduced in the cell, the product of the second reduction could not be reoxidized to yield fully the spectrum of the precursor complex. The product of controlled-potential electrolysis at −1.2 V (0 °C) showed a weak ($\epsilon \sim 5$ M^{-1} cm^{-1}) band near 600 nm and an intense charge transfer extending well into the visible region; however, it is unlikely that this is an accurate spectrum, due to the chemical decomposition processes.
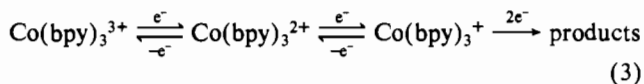
Discussion

Cobalt(III) complexes with unidentate or multidentate amine ligands are kinetically inert (d^6, low spin) and undergo initial 1-e reductions to labile cobalt(II) (d^7, high spin) with varying degrees of reversibility.[10] These initial reductions are invariably followed by an irreversible 2-e reduction at more negative potentials to cobalt metal (eq 1). The intermediate

$$\text{Co(III)} \underset{-1e^-}{\overset{1e^-}{\rightleftarrows}} \text{Co(II)} \xrightarrow{2e^-} \text{Co(0)} \qquad (1)$$
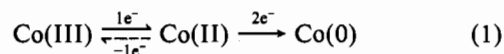
oxidation state cobalt(I) (d^8) has been identified, however, in complexes with macromonocyclic,[5] Schiff's base,[11] dimethylglyoximato,[12] or vitamin B$_{12}$[13] type ligands, where stereochemical change involving loss of axial ligands also occurs (eq 2). With Co(bpy)$_3^{3+}$ (bpy = 2,2′-bipyridyl), several
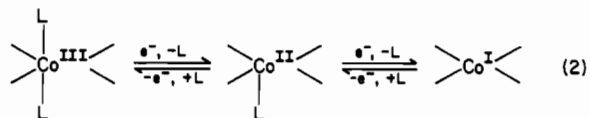
reversible reductions occur without stereochemical change, involving both cobalt(II) and cobalt(I) species (eq 3).[14]

$$\text{Co(bpy)}_3^{3+} \underset{-e^-}{\overset{e^-}{\rightleftarrows}} \text{Co(bpy)}_3^{2+} \underset{-e^-}{\overset{e^-}{\rightleftarrows}} \text{Co(bpy)}_3^+ \xrightarrow{2e^-} \text{products} \qquad (3)$$

An extensive study of the macrobicyclic complexes based on the parent ligands 3,6,10,13,16,19-hexaazabicyclo[6.6.6]-

(10) Vlcek, A. A. *Prog. Inorg. Chem.* **1963**, *5*, 211. Bond, A. M.; Keene, F. R.; Rumble, N. W.; Searle, G. H.; Snow, M. R. *Inorg. Chem.* **1978**, *17*, 2847.
(11) Averill, D. F.; Broman, R. F. *Inorg. Chem.* **1978**, *17*, 3389.
(12) Schranzer, C. N. *Angew. Chem., Int. Ed. Engl.* **1976**, *15*, 417.
(13) Brown, D. G. *Prog. Inorg. Chem.* **1973**, *18*, 177.
(14) Tanaka, N.; Sato, Y. *Bull. Chem. Soc. Jpn.* **1968**, *41*, 2059. Szalda, D. J.; Creutz, C.; Mahajan, D.; Sutin, N. *Inorg. Chem.* **1983**, *22*, 2372.

icosane (sar) and 3,6,10,13,15,18-hexaazabicyclo[6.6.5]nonadecane (absar) has been reported recently.[3] Invariably, the compounds displayed a reversible 1-e couple, followed by an irreversible reduction below −2 V. The nature of the ligands effectively traps the metal ion in the ligand cavity, rendering the cobalt(II) ion inert to substitution and enforcing the six-coordinate geometry.[15] The second irreversible reduction occurs at appreciably more negative potentials than those observed with normal multidentate amine complexes and involves C–N bond rupture of the macrobicyclic cage. Only with unsaturated macrocyclic imine ligands is the cobalt(I) oxidation state inferred,[16] and it is presumed that the stability of this enforced six-coordinate cobalt(I) species is related to considerably back-donation of electron density from the metal to the imine ligands, analogous to the $Co(bpy)_3^+$ case.

For the sar ligands, molecular-mechanics calculations indicate that the cavity can best accommodate an ion intermediate in size to the cobalt(III) and cobalt(II) ions.[17] The larger Co(I) ion may not be readily accommodated. However, the mixed amine–thioester sar complexes investigated in this study have an appreciably larger cavity than the hexaamine sar ligands, as a consequence of the longer C–S (1.80 Å)[7] compared with C–N bonds (1.48 Å)[18] in the two analogues. This aspect alone may help stabilize lower oxidation states. Further, there exists the prospect of delocalizing electron density over the thioether donor atoms from the metal ion, since thioether radicals are appreciably more stable than amine radicals.[19]

The macrobicyclic complexes with amine and thioether donors (II, IIIa,b) clearly involve sequential 1-e steps to well-characterized stable cobalt(II) species and subsequently to apparently cobalt(I) species. The uncapped precursor sexidentate complex $Co(ten)^{3+}$ displayed the initial 1-e reduction followed by a second reduction step that varied from one electron to two electrons in character depending on the solvent. However, on the coulometric time scale only the Co(II)/Co(0) 2-e reduction was observed for $Co(ten)^{3+}$ in both aqueous and aprotic solvents. Evidently, encapsulation contributes to the stability of the cobalt(I) oxidation state, probably by impeding dissociative reactions. No further metal-centered reductions beyond Co(I) were observed for the N_3S_3 macrobicyclic complexes even in aprotic solvents before the solvent limit. Nor were any oxidations of the Co(III) center observed.

The electrochemistry of the azacapten complex alone is complicated by adsorption phenomena[20] at Hg for the Co(II)/Co(I) reduction and also by a multielectron reduction in both aqueous and aprotic solvents near the solvent limit. Cathodic reductions of organic sulfonyl, sulfinyl, sulfonium, and thioethers have been reported at potentials in the range −1.5 to −2.5 V.[21,22] Generally, 1-e reductions to relatively long-lived radical anions precede a further 1-e addition that leads to irreversible C–S bond cleavage. The radical intermediate may alternatively react with water or dimerize. Presumably the multielectron wave at very negative potentials

observed in the complexes involves such ligand-centered rather than metal-centered processes. This chemistry is not germane to the metal-centered behavior and has not been pursued exhaustively at this stage.

The two 1-e metal-centered processes observed lead to hexacoordinate cobalt(II) and cobalt(I) ions. The cobalt(II) ion was readily prepared and isolated by reduction with zinc dust and has been characterized spectroscopically previously[7] as low-spin cobalt(II) from magnetic moment measurements.[23] Visible absorption spectroscopy and an X-ray crystal structure analysis[18] clearly indicate the ion is essentially six-coordinate cobalt(II). The ESR spectrum of the $Co((NH_3^+)capten)^{3+}$ complex determined at 4.2 K exhibits g values of 1.94, 2.21, and 4.22 and differs somewhat from the spectrum of high-spin hexaamine macrobicyclic cobalt(II) ions.[24] Apart from the macrobicyclic complexes, cobalt(II) species are not generally six-coordinate, preferring five-coordinate geometry. To the best of our knowledge, the spectrum (Figure 7) represents the first ESR of a characterized sexidentate, low-spin cobalt(II) complex ion.

The apparently d^8 cobalt(I) ion is not chemically stable on a coulometric time scale at room temperature. However, its in situ generation at −60 °C and subsequent trapping in the solvent glass at 100 K allowed a spectrum to be recorded rapidly. An eight-line pattern ($g = 2.17$, $A = 67$ G; Figure 8) was observed. Any signal from cobalt(II) is broad and weak at this temperature and hence does not interfere. Electrolysis conditions were chosen to limit cobalt(II) as a contaminant, and later reoxidation and spectroscopic analysis indicated negligible decomposition in the time scale of the experiment.

We have reviewed the reduced ion in three ways: (i) a d^8 cobalt(I) ion, with the unpaired electron density residing essentially on the metal ion; (ii) a d^7 cobalt(II)–thioether radical species, where the unpaired electron density resides entirely on a thioether donor; (iii) an intermediate configuration, where partial back-donation of electron density from the metal ion over the thioether donor atoms occurs. The observed eight-line pattern clearly indicates a hyperfine interaction with the cobalt ion. The g value of 2.17 is distinctly different from the free electron value usually observed for organic radical species or metal complexes where the unpaired electron density resides dominantly on the ligand, implying appreciable metal involvement with the unpaired electron density. The coupling constant of 67 G is similar to the coupling constant observed for low-spin five-coordinate cobalt(II)–sulfide species (53 G) where the conclusion was that the odd electron density resided in a molecular orbital with appreciable metal $3d_{xy}$ orbital character, although a significant amount of 3d–4p hybridization was invoked along with some appreciable covalent character in the designated orbital.[25] The binuclear anion $[\eta^5\text{-}C_5H_5Co(CO)]_2^-$ also displays a 15-line ESR signal with $A_{iso} = 50$ G, and X-ray structural evidence is fully consistent with the electron equally distributed between the two cobalt atoms in metal d orbitals.[26]

Spectra of octahedral d^8 Ni^{2+} doped in single crystals of ESR-inactive salts frequently exhibit single absorption lines at low temperature; for example, Ni^{2+} doped in $M(NO_3)_2\cdot 6NH_3$ (M = Zn, Cd) showed single lines at $g = 2.17$, analogous to the $g = 2.18$ observed for single crystals of $Ni(NO_3)_2\cdot 6NH_3$.[27]

(15) The sexidentate nature of the cobalt(II) state has been established by crystal structure analysis for both hexaaza and trithiatriaza cages: Snow, M. R.; Hambley, T. W., unpublished results. See also ref 3.
(16) Larsen, E.; La Mar, G. N.; Wagner, B. E.; Parks, J. E.; Holm, R. H. *Inorg. Chem.* **1972**, *11*, 2652.
(17) Reference 6. However, calculations have not been performed for the trithiatriaza cages at this stage.
(18) Hambley, T. W.; Snow, M. R., unpublished structural data.
(19) Kochi, J. K. "Free Radicals"; Wiley: New York, 1973; Vol. II.
(20) Laviron, E. In "Electroanalytical Chemistry"; Bard, A. J., Ed.; Marcel Dekker: New York, 1982; pp 53–158.
(21) Howsam, R. W.; Stirling, C. J. M. *J. Chem. Soc., Perkin Trans. 2* **1972**, 847. Moiroux, J.; Fleury, M. B. *Electrochim. Acta* **1973**, *18*, 691. Fischer, C. M.; Erickson, R. E. *J. Org. Chem.* **1973**, *38*, 4236.
(22) Lamm, B.; Samuelsson, B. *Acta Chem. Scand.* **1970**, *24*, 561.

(23) Dubs, R. V.; Gahan, L. R.; Sargeson, A. M., submitted for publication in *Aust. J. Chem.*
(24) Comba, P.; Lawrance, G. A.; Martin, L. L.; Sargeson, A. M., unpublished data.
(25) Genser, E. E. *Inorg. Chem.* **1968**, *7*, 13.
(26) Schore, N. E.; Ilenda, C. S.; Bergman, R. G. *J. Am. Chem. Soc.* **1976**, *98*, 255.
(27) Ochi, J. A.; Sano, W.; Isotani, S.; Hennies, C. E. *J. Chem. Phys.* **1975**, *62*, 2115.

The implication from these comparisons is that there is appreciable metal character in the unpaired electron density. Some radical character is implied indirectly from the limited chemical stability of the cobalt(I) species, since such species are likely to undergo irreversible chemical reactions with solvent.[19,21,22] The ability to delocalize some electron density onto the thioether donors is also likely to be the key to the different redox chemistry between CoN_6 and CoN_3S_3 macrobicyclic complexes.

Notes

Contribution from the Department of Chemistry, Technion—Israel Institute of Technology, Haifa 32000, Israel, and Institute of Inorganic Chemistry, University of Frankfurt, D-6000 Frankfurt, West Germany

On the Nonobservability of Cubic P8

E. Amitai Halevi,[1a] Hans Bock,*[1b] and Bernhard Roth[1b]

One of the more perplexing features of the chemistry of elemental phosphorus is the absence of any P_6 or P_8 species from the manifold of its allotropic forms.[2] This point has been underscored in a recent photoelectron spectroscopic investigation of the equilibrium $P_4 \rightleftharpoons 2P_2$.[3] No other species was detected in the vapor phase up to 1470 K. Specifically, P_8, the expected product of the dimerization of P_4, and P_6, which might be formed by the addition of P_2 to P_4, were conspicuously absent.

Exploratory semiempirical computations, using MNDO,[4] disclosed a number of P_6 and P_8 species, each at a minimum in the potential energy surface; several of them are calculated to be thermodynamically more stable than their dissociation products. The failure to observe any particular one of them could arise from either of two causes: (1) An insurmountable kinetic barrier prevents its formation. (2) Although it may be formed with relative ease, it is immediately converted to some more stable species; in the present instance, this would presumably be $(P_4)_n$, i.e. common red phosphorus.
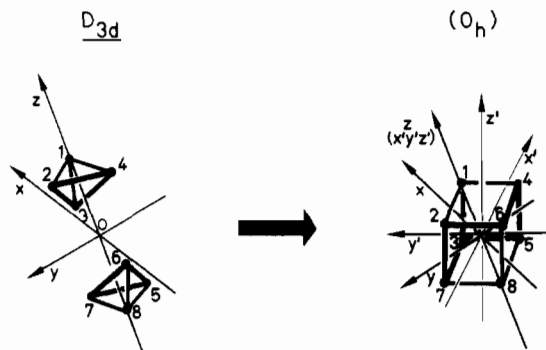
In this paper we consider the most stable of these molecules, cubic (O_h) P_8. Possible pathways leading to other P_8 and P_6 species are presently being explored.

Ground-State Energies and Geometries

The calculated energies and geometries of P_2, P_4, and P_8 are summarized in Table I.

The reliability of the computational method is confirmed by the good agreement of the value ($\Delta H° = 43$ kcal/mol) calculated for the equilibrium $P_4 \rightleftharpoons 2P_2$. The temperature dependence of the equilibrium constant yields $\Delta H° = 55$ kcal/mol over the range 1170–1470 K,[3] whereas the best thermochemical value in this temperature range is 53 ± 1 kcal/mol.[5]

The value ($\Delta H° = -68$ kcal/mol), calculated for the equilibrium $2 P_4 \rightleftharpoons P_8$, leaves no doubt that cubic P_8 is substantially more stable than two tetrahedral P_4 molecules, as simple considerations of steric strain would suggest. Our

(1) (a) Technion—Israel Institute of Technology. (b) University of Frankfurt.
(2) See, e.g., Figure 8 of: Corbridge, D. E. C. "The Structural Chemistry of Phosphorus"; Elsevier: Amsterdam, 1974; p 22.
(3) Bock, H.; Müller, H. *Inorg. Chem.*, companion article in this issue.
(4) Dewar, M. J. S.; Thiel, W. *J. Am. Chem. Soc.* **1977**, *99*, 4899, 4907.
(5) "JANAF Thermochemical Tables"; Dow: Midland, MI 1960.

Figure 1. Highest symmetry reaction path (D_{3d}) for dimerization of tetrahedral P_4 to cubic P_8. Bonds broken: (23), (34), (42), (56), (67), (75). Bonds made: (26), (64), (45), (53), (37), (72).

Table I. Calculated Enthalpies of Formation and Bond Lengths of Various Species of Elemental Phosphorus

species	symmetry	ΔH_f, kcal	r_{PP}, Å calcd	r_{PP}, Å exptl
P_2	$D_{\infty h}$	40.7	1.693	1.894
P_4	T_d	36.2	2.052	2.21
P_8	O_h	4.1	2.074	

results are confirmed to some extent by Trinquier, Malrieu, and Daudey,[6] who performed ab initio pseudopotential SCF calculations employing double-ζ basis sets and found (without inclusion of d polarization functions) cubic P_8 to be more stable than two P_4 by 10 kcal/mol. They are in conflict with those of Fluck, Pavlidou, and Janoschek,[7] who find P_8 to be unstable with respect to two P_4 molecules by some 47 kcal/mol. These authors did not optimize the P–P distance for P_8 but used the experimental value in P_4 for both molecules. It is clear from the table that, although bond lengths calculated by MNDO are consistently shorter than the experimental ones, the P–P bond is appreciably longer in P_8 than in P_4. It follows that the energy calculated for the former at the experimental bond length of the latter is necessarily too high.

Qualitative Symmetry Analysis (OCAMS)

The cubic P_8 molecule has O_h symmetry. If it is stretched along one of its diagonals, its symmetry is reduced to D_{3d}. Further elongation of the diagonal, with retention of D_{3d} symmetry, eventually produces two P_4 molecules, so orbital correspondence analysis in maximum symmetry (OCAMS)[8] is carried out in D_{3d}, the highest symmetry compatabile with

(6) Trinquier, G.; Malrieu, J.-P.; Daudey, J.-P. *Chem. Phys. Lett.* **1981**, *80*, 552.
(7) Fluck, E.; Pavlidou, C. M. E.; Janoschek, R. *Phosphorus Sulfur* **1979**, *6*, 469.
(8) (a) Halevi, E. A. *Helv. Chim. Acta* **1975**, *58*, 2136. (b) Katriel, J.; Halevi, E. A. *Theor. Chim. Acta* **1975**, *40*, 1.